IEEE Access
Multidisciplinary | Rapid Review | Open Access Journal

SPECIAL SECTION ON TOWARDS SERVICE-CENTRIC INTERNET OF THINGS (IOT): FROM MODELING TO PRACTICE

Received September 30, 2018, accepted October 21, 2018, date of publication December 3, 2018,
date of current version December 27, 2018.

Digital Object Identifier 10.1109/ACCESS.2018.2883737

Noise Analysis and Modeling in Visible Light Communication Using Allan Variance

LUCHI HUA[1], YUAN ZHUANG[1,2], (Member, IEEE), LONGNING QI[1], JUN YANG[1], (Member, IEEE), AND LONGXING SHI[1], (Senior Member, IEEE)

[1]Southeast University, Nanjing 210096, China
[2]Bluvision Inc., Fort Lauderdale, FL 33334, USA

Corresponding author: Yuan Zhuang (zhy.0908@gmail.com)

This work was supported by the National Natural Science Foundation of China under Grant 61771135 and Grant 61574033, and the National Science and Technology Major Project of China under Grant 2017ZX01030101-002.

ABSTRACT Visible Light Communication (VLC) is a rising communication technology which uses Light-Emitting Diode (LED) luminaries for high-speed data transferring; however, the optical signal is usually degraded by the noise in the practical VLC system. In this paper, Allan Variance is introduced for noise analysis and modeling in VLC for the first time, which provides an efficient method to measure different kinds of noise in the VLC systems. By applying Allan variance to analyze the signals collected from the real-world environment, both white noise and random walk are observed in the VLC systems. The observed white noise and random walk are also modeled by using the Allan variance. The noise analysis and modeling based on Allan variance provide a method to improve the performance of VLC.

INDEX TERMS Visible light communication (VLC), Allan Variance, white noise, random walk, time-correlated noise, photodiode.

GLOSSARY

FFT	Fast Fourier Transform
LED	Light-Emitting Diode
LiFi	Light Fidelity
MCU	Microcontroller Units
PWM	Pulse Width Modulation
PSD	Power Spectral Density
SNR	Signal-to-Noise Ratio
VLC	Visible Light Communication
VLP	Visible Light Positioning

I. INTRODUCTION

Visible Light Communication (VLC) is a rising communication technology which uses Light-Emitting Diode (LED) luminaries for high-speed data transferring. During past decades, there are various applications using VLC technology, such as Light Fidelity (LiFi) [1] and Visible Light Positioning (VLP) [2]. As an environmentally-friendly lighting source, LED has become prevalent among publics. The benefit of a VLC system comes in many ways, such as high rate transmission [3], energy saving, long lifetime, low maintenance cost [4], and less heating. In addition, since the visible light band is far away from the electromagnetic waves, it cannot produce electromagnetic interference, which is quite safe for hospitals with large amounts of equipments. In positioning application area, popular solutions such as WiFi and Bluetooth are severely affected by multipath interference [5], [6]. Fortunately, visible light energy is largely degraded by distance and large incident angles that most reflections will not affect line-of-sight signals.

Albeit those advantages of the visible light signals, it is important to improve the quality of the optical signal to achieve higher performance in visible light systems. The received signal strength (RSS) is widely researched in VLC studies because it directly indicates the signal quality [7], [8]. Many RSS-based applications are often found in VLP related researches [2], where high accurate RSS is demanded. The VLP system is developed to estimate the location of the receiver (e.g., photo-detector, camera, etc.). RSS has a great influence on the VLC applications because an inaccurate RSS may result in failure in detecting objects and further cause communication outages [9].

A. NOISE IN VLC SYSTEM

Currently, the VLC system mainly focuses on two kinds of noise: 1) shot noise and 2) thermal noise [10].

1) **Shot noise** is mainly generated by LED lights and the ambient light in the PIN tube. Firstly, the white LED cannot filter out the interference of the modulated visible lights with a band-stop filter, and the LED lamp is controlled by the bias voltage. Therefore, there is a small amount of power

output even at a low level which may result in the noise in the receiver. This is the noise generated by the LED itself. Secondly, there is a large amount of visible light in the sunlight, which is inevitably received by the detector. For some artificial light sources (e.g., fluorescent lamps, incandescent lamps, etc.), their emitted optical power will affect the detector. Some of these light sources are often modulated at a frequency of 50 Hz, while others (e.g., fluorescent lamps) are modulated at hundreds of kHz, which may influence on the modulation signal of the LED itself. Shot noise introduced by these noise sources is often referred as an additive white noise in the literature [11].

2) **Thermal noise** is mainly generated by the amplifier and loaded in the receiver. It is mainly caused by free electrons or charge carriers inside the resistor for irregular thermal motion. If there is no external field, the electrons in the conductor do irregular thermal motion and have no directional migration, thus causing no current. However, due to the fluctuations in the real world, the number of electrons moving in two opposite directions is not completely equal. This effect results in an increase or fall of the voltage in conductors and semiconductors, which is also called the noise voltage, producing noise current. The mean square value of the thermal noise consists of feedback resistor noise and FET noise [11].

B. NOISE ANALYSIS FOR VLC SYSTEM

How the noise affects the performance of visible light systems has been studied for decades. As discussed in the previous subsection, typical noises in VLC receivers are shot noise and thermal noise due to the p-n junctions in the circuits of the receivers [12], [13]. The study [11] presents that a large noise can degrade the signal-to-noise ratio (SNR) and further decrease the data rate of the VLC. In the research [14], various parameters of the noise model were studied to learn their influence on the VLC systems. In the research [10], the interference of different LEDs was studied. The noise was determined by noise modeling based on background current measured, which was measured by a specific instrument.

C. NOISE ANALYSIS USING ALLAN VARIANCE

Developed in the 1960s, the two-sided Allan variance was initially used to study the frequency stability of the oscillator in the clock system [15]. Decades later, researches applied it to study the error characteristics of the inertial sensor [16]. In 1999, IEEE published a standard [17] to illustrate the process of using Allan variance to analyze inertial sensors. In this century, the Allan variance was introduced in GNSS studies to identify the error characteristics of GNSS solutions [18]. The research [18] found out a list of main noise in the GNSS system, which are the first-order Gaussian Markov process, white noise, random walk, and flicker noise. The use of the Allan variance for colored noise analysis was introduced recently [18]. The paper studied colored noise produced by fading and shadowing in wireless communication systems.

D. MAIN CONTRIBUTION OF THIS PAPER

Previous works typically assume the noise in the VLC system are shot noise and thermal noise and model the noise by using Gaussian white noise. And, most researches only have simulation results rather than experimental studies. This paper uses Allan variance to analyze and model the noise of the VLC system and finds white noise and time-correlated noise are existed in the VLC system by experimental studies. The time-correlated noise is detected in the VLC system for the first time.

II. ALLAN VARIANCE

Different from calculating root mean squares (RMS) or frequency domain methods, the Allan variance is a time-series analysis method to extract the noise from the data. It expresses the root mean squares error varied with time. The specific principles of the Allan variance are given as follows [16].

For a random process $X(t)$, data is measured at discrete times with the sampling interval t_0, that is $t = kt_0$, $k = 1, 2, 3, ..., N_s$. Reminding that in the Allan variance, a cluster refers to a set of consecutive sampling points. First, suppose $n(n < N_s/2)$ sampling points, sum of which is a total time length τ, is used as a cluster, then the total number of clusters is the integer of N_s divided by n. The mean value of two adjacent clusters are given by:

$$\bar{X}_k(n) = \frac{1}{n}\sum_{i=k}^{k+n-1} X_i \tag{1}$$

and

$$\bar{X}_{k+n}(n) = \frac{1}{n}\sum_{i=k+n}^{k+2n-1} X_i \tag{2}$$

Second, calculate the difference between every two adjacent data clusters:

$$\xi_{k+n,k} = \bar{X}_{k+n}(n) - \bar{X}_k(n) \tag{3}$$

The Allan variance of a cluster with the length of τ ($\tau = n \cdot t_0$) can be represented by:

$$\sigma^2(\tau) = \frac{1}{2}\left\langle \xi^2_{k+n,k} \right\rangle \tag{4}$$

That is:

$$\sigma^2(\tau) = \frac{1}{2(N_s - 2n + 1)}\sum_{k=1}^{N_s-2n+1}\left(\bar{X}_{k+n}(n) - \bar{X}(n)\right)^2 \tag{5}$$

For random process $X(t)$, its power spectral density (PSD) is represented by $S_X(f)$. The unique relationship between the Allan variance and the PSD is:

$$\sigma^2(\tau) = 4\int_0^\infty S_X(f)\frac{\sin^4(\pi f\tau)}{(\pi f\tau)^2}df \tag{6}$$

Finally, by using the same process, the Allan variance for other cluster length is calculated. Therefore, the final result is the Allan variance versus cluster length.

A. ALLAN VARIANCE OF BASIC NOISES

In IEEE standard [19], quantization noise, white noise, random walk and other spectral noise components are described by different PSD laws. This allows to distinguish those noises by the slope of the curve in a log–log plot (Allan variance versus cluster length), as shown in Fig. 1. The figure shows a combined result of all basic noises in inertial sensor. However, it is readily to identify each noise in particular time region. The curve begins with quantization noise with the slope of -1, then white noise part with the slope of $-1/2$. It ends with Random walk and drift ramp, with the slope of 1/2 and 1 respectively. The magnitudes of these noises are easy to calculate as soon as the relationship of the PSD and the Allan variance is established. The characteristics and calculation of the noises found in a practical visible light system are given in the next part.

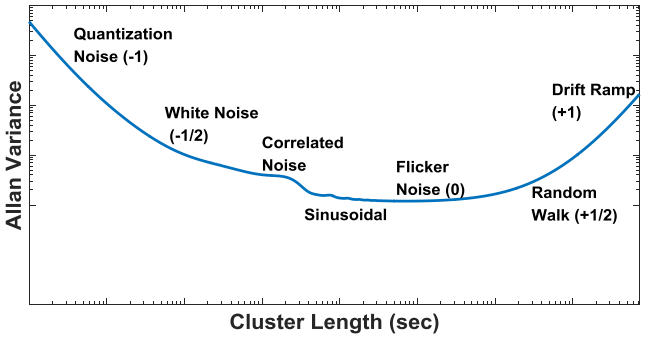

FIGURE 1. Allan variance analysis results of basic noises [19].

1) WHITE NOISE

In most VLC studies, the white noise refers to shot noise and thermal noise [10], [11], [14]. More explicitly, the shot noise are caused by dark current of photo detector, illuminance of LED, and illuminance of ambient light. Fluctuation of the LED signal can also be treated as white noise [20], [21]. This fluctuation is usually due to the unstable power supply and modulation of the LED.

The Allan variance for Gaussian white noise is given in IEEE standard [19] as:

$$\sigma^2(\tau) = \frac{N^2}{\tau} \tag{7}$$

where N is the coefficient for white noise. From Eq. (7), in the log-log plot, the slope of the Allan variance curve is $-1/2$. N can be calculated by:

$$N = \sigma(1) \tag{8}$$

Fig. 2 shows the relationship between PSD and Allan variance of the Gaussian white noise.

2) RANDOM WALK

In practical system, the signal not only suffers from white noise, but also from time correlated perturbation. The random walk is a noise with very long time correlation which origins

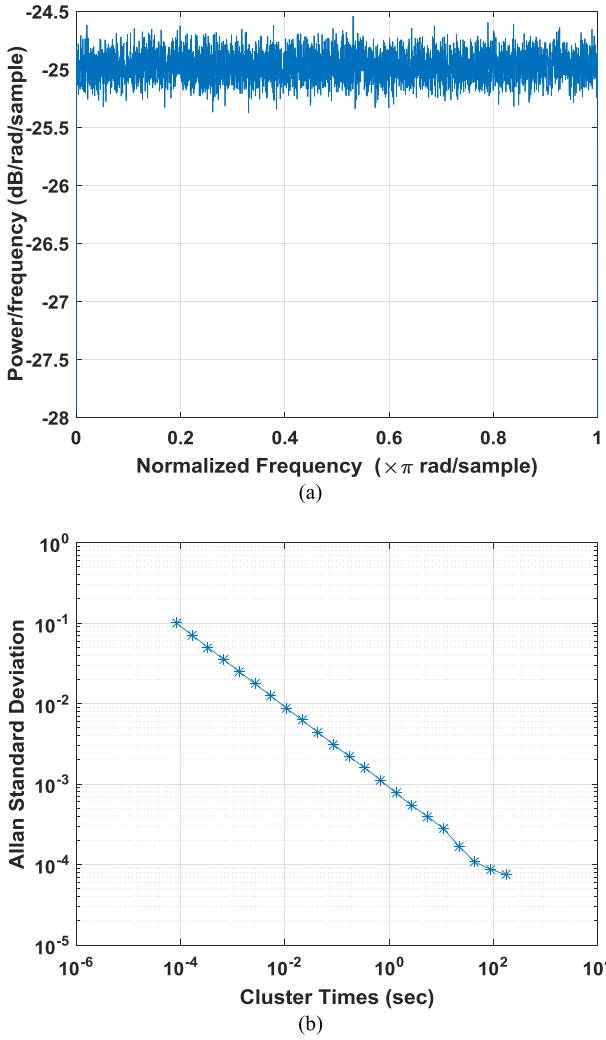

FIGURE 2. Power spectral density and Allan variance of a signal with Gaussian white noise. (a) Power spectral density and (b) Allan variance.

from the Brownian motion in the receiver circuit [22]. The Allan variance of random walk is given by:

$$\sigma^2(\tau) = \frac{K^2\tau}{3} \tag{9}$$

where K represents the random walk coefficient. The curve slope of the Allan variance is $+1/2$. The value of K is represented by:

$$K = \sigma(3) \tag{10}$$

The simulated results of a signal with random walk are shown in Fig. 3.

3) OTHER NOISES

Other noises such as drift ramp and flicker noise have not yet been identified in our results. Some noises such as quantization noise and correlated noise (1st order Gaussian Markov Noise) are unstable and too obscure to identify. Experiments will continue in future to study those noises. The Allan variance results of some basic noises are given in TABLE 1 [19].

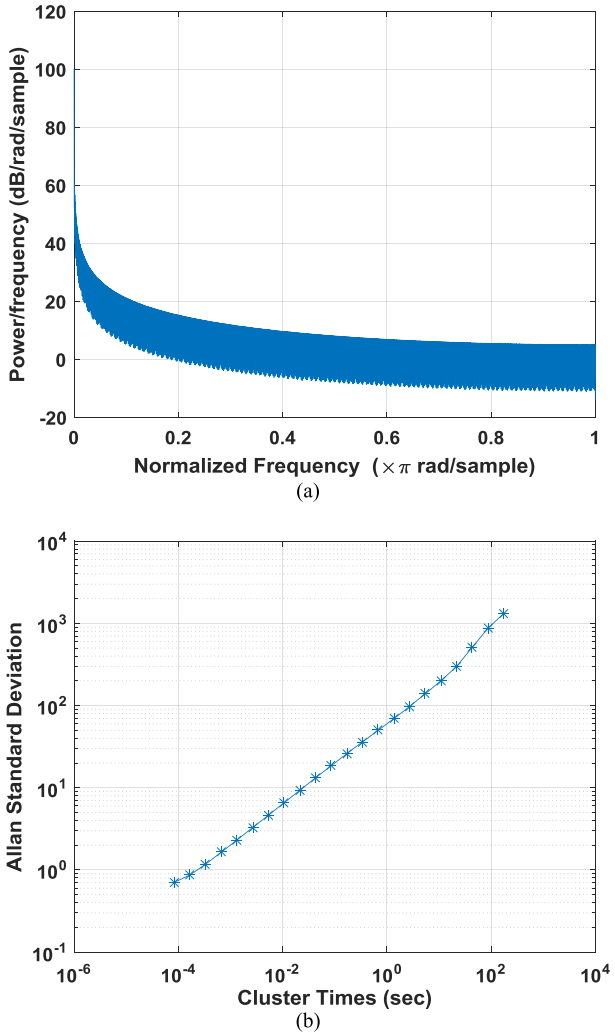

FIGURE 3. Power spectral density and Allan variance of a signal with random walk. (a) Power spectral density and (b) Allan variance.

TABLE 1. Parameter settings of the system environment.

Noise	Allan variance	Slope	Coefficient Value
Quantization Noise	$\frac{3Q^2}{\tau^2}$	-1	$Q=\sigma\ \sqrt{3}$
Flicker Noise	$\frac{2B^2\ln 2}{\pi}$	0	$B=\sigma\ f_0$
Rate Ramp	$\frac{R^2T^2}{2}$	$+1$	$R=\sigma\ \sqrt{2}$
White Noise	$\frac{N^2}{T}$	$-\frac{1}{2}$	$N=\sigma\ 1$
Random Walk	$\frac{K^2\tau}{3}$	$+\frac{1}{2}$	$K=\sigma\ 3$

B. ACCURACY OF ALLAN VARIANCE

The accuracy of the calculated Allan variance is related to the cluster number involved in the calculation. The percentage error δ of the Allan variance estimation for a specific cluster length T is expressed as follows. If the percentage error is defined as:

$$\delta = \frac{\sigma(\tau, M) - \sigma(\tau)}{\sigma(\tau)} \tag{11}$$

where M is the number of clusters, $\sigma(\tau, M)$ is the Allan variance for M clusters. This equation is equal to [23]:

$$\sigma(\delta) = \frac{1}{\sqrt{2\left(\frac{N_s}{n} - 1\right)}} \tag{12}$$

Eq. (12) shows that the accuracy of the Allan variance is better with a longer sampling time. For example, when the cluster length is 1 second, the percentage error of a 24-hour consecutive data is 0.24%. However, a 1-minute data gives 9.21% percentage error. In this paper, each set of data is collected for 20 minutes, and the RSS is provided by FFT method for each 1/600 second, which gives the percentage error of 0.08%.

III. APPLICATION TO VLC

The performance of the visible light system is affected by white noise and other noises. These noises can be treated as random processes. In this paper, a very convenient noise analysis method, the Allan variance method, is used to qualitatively analyze these noises. The Allan variance directly observes the different noises in the system and learns the coefficient of each noise. Although related papers have pointed out that the shot noise in the photoelectric sensor has the most significant influence on the signal in the visible light system [11], [24], it is uncertain to neglect other the noises in a practical environment where exists more complex signal propagations. Therefore, we build a practical visible light system and the Allan variance will be performed to study all potential noise sources in the collected data including white noise and time-correlated noise.

A. SYSTEM STRUCTURE

The relationship between the Allan variance method and our visible light system is shown in Fig. 4. The visible light system is separated into two modules: transmitter module and receiver module. The transmitter module configures the control parameters, which mainly include Pulse Width Modulation (PWM) waves-related parameters such as modulation frequency and duty cycle. Meanwhile, photodiode,

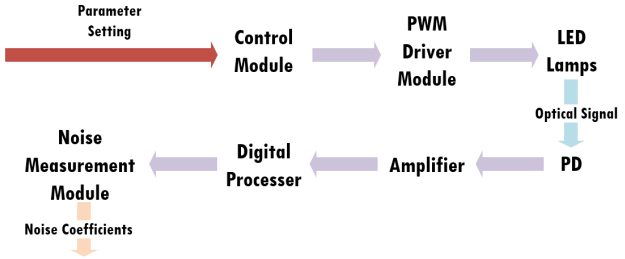

FIGURE 4. The system structure of the visible light system.

amplifier, digital processor, and noise measurement module are included in the receiver module. The optical signal from the transmitter module is received by the photodiode in the receiver. The signal amplifier of the receiver module includes the inherent module circuit and the external adjustment circuit. The digital processor performs the operations of windowing and Fast Fourier Transform (FFT) transformation and finally provides the RSS values corresponding to the modulated LED. The received signal from the photodiode is processed by the signal amplifier and digital processor and then sent to noise measurement module and noise mitigation module. The noise measurement module estimates all identified noise through Allan variance and output the coefficient of each noise.

B. TEST ENVIRONMENT

The field test environment, as shown in Fig. 5(a) was arranged in a large office in Sensors Center, Southeast University, Wuxi, China. The parameter settings of the system environment are summarized in Table 2. Since all experiments were conducted at night, the sunlight interference was avoided.

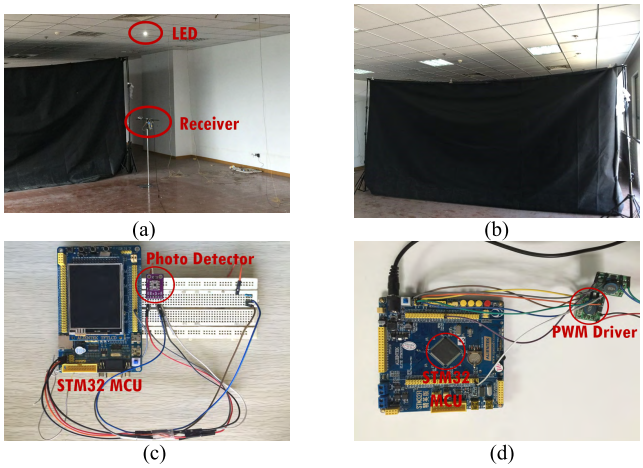

FIGURE 5. Field setup of the visible light system. (a) General view of the system; (b) Darkroom for field tests; (c) Transmitter module; (d) Receiver module.

TABLE 2. System settings.

Parameter	Value
Cell size (L×W×H)	5m×5m×2.843m
Environment temperature	-2~3℃
LED power (P_T)	10W
LED location (x, y, z) (m)	(2.5, 2.5, 2.828)
Modulated frequencies	5kHz (3.2kHz, 4.5kHz)
Duty cycle	70%
Height of the receiver	1.25m
Effective area of the photodiode	5.2mm^2
Responsivity	135mA/W
Bandwidth	48kHz
Dark current	2.5pA

A relatively large experimental environment sized $5 \times 5 \times 2.843$ m^3 was surrounded by a background cloth bracket, which is illustrated in Fig. 5(b). It is because disturbance factors such as the ambient light from outside of the window should be avoided as much as possible in the experiments. With this black background cloth, most of the lights that hit its surface can be absorbed. Therefore, the streetlights outside the window could not enter or affect the experimental environment.

We used a photodetector modeled Texas Instrument OPT101 in the receiver, as shown in Fig. 5(c). A STM32 development board was used for signal processing. The embedded AD module in the STM32 board receives analog signal from the photodetector. All Data are stored on an inserted SD card.

The transmitter connection is shown in Fig. 5(d). We used a photodiode modeled Texas Instrument OPT101 in the receiver, as shown in Fig. 5(d). PWM wave, which was output by the TIMER of the STM32 Microcontroller Units (MCU), was used to modulate a 10W LED lamp. To follow the Nyquist sampling law, since our system is limited by the sampling rate of 12 kHz, the frequencies should not be set above 6 kHz. The duty ratio was 70% in this test.

IV. RESULTS AND ANALYTICS

A. DARK CURRENT NOISE OF THE RECEIVER

The parameters for the field test are shown in Table 2 and the test was conducted during the night in the darkroom. The first test was conducted with LED turned off. Therefore, the signal received was generated by the dark current of the receiver. The Allan variance of the signal was shown in Fig. 6. It can be observed from the result that the main noise type is white noise because dark current noise is one of the sources for shot noise. The yellow line which stands for the Gaussian white noise fits the left half of the Allan variance curve by using the least squares to minimize the fitting error. The red line stands for the fitting line combined two type of noise or more, which will be easy to understand in the next test. The coefficient of white noise was found to be 0.01093.

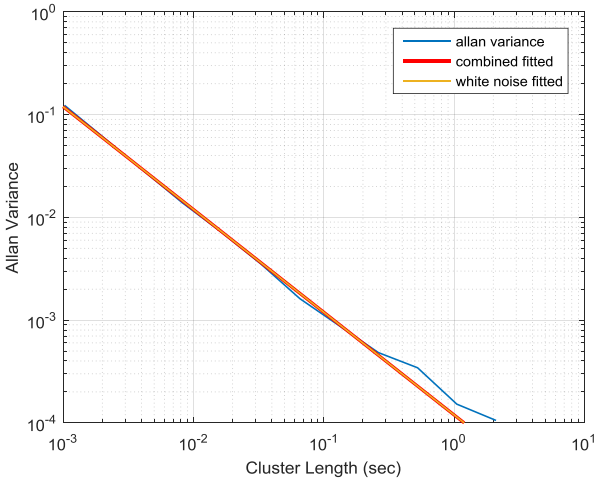

FIGURE 6. Allan variance of the RSS values received under the conditions of no LED on.

B. VLC NOISE IN INTERFERENCE-FREE ENVIRONMENTS

In this test, the LED was turned on and modulated in 5 kHz. Also, there was no other ambient light interference. The result of Allan variance is illustrated in Fig. 7. In Fig. 7, the left curve shows the characteristic of white noise while the right curve obviously shows the random walk. Moreover, the coefficient of the white noise is large than that of the condition when the LED is off. Since there was no ambient light interference, we also checked the Allan variance of the same signal but not on the modulated frequency. We used the RSS value on 1.8 kHz, 2.5 kHz, 3.2 kHz, and 4.5 kHz and performed the Allan variance method. The fitting results of the curves are shown in Fig. 8 and Fig. 9 and the extracted coefficient are shown in TABLE 3. It can be seen that when there is no ambient light or other LED sources, the noise only consists of white noise. However, the coefficients of the white noise are large than that of the condition when the LED is off. It shows that the illuminance of the LED influences the whole frequency spectrum.

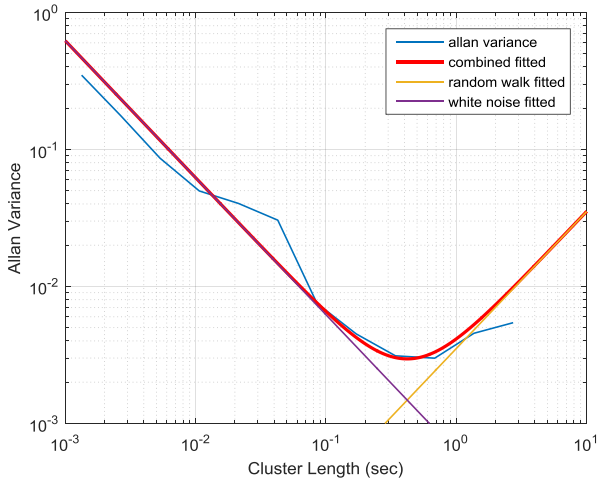

FIGURE 7. Allan variance of the RSS values received from one LED (5 kHz) under the conditions of only one LED on and no ambient light interference.

TABLE 3. Noise of received signal on different frequencies.

LED	White Noise (N)	Random Walk (K)
5 kHz	0.02493	0.10276
4.5 kHz	0.01391	N/A
3.2 kHz	0.01538	N/A
2.5 kHz	0.01509	N/A
1.8 kHz	0.01429	N/A

In order to check that the random walk is not an occasion, we conducted another two tests, using two LEDs with the same model but modulated in different frequencies (3.2 kHz, 1.8 kHz). The Allan variance results of these two tests are shown in Fig. 10 and Fig. 11 and the coefficients are listed in TABLE 4. The random walk is found in both results. Therefore, the random walk would not be negligible. While white noise contributes most on the short clusters, the random walk influences on the long term.

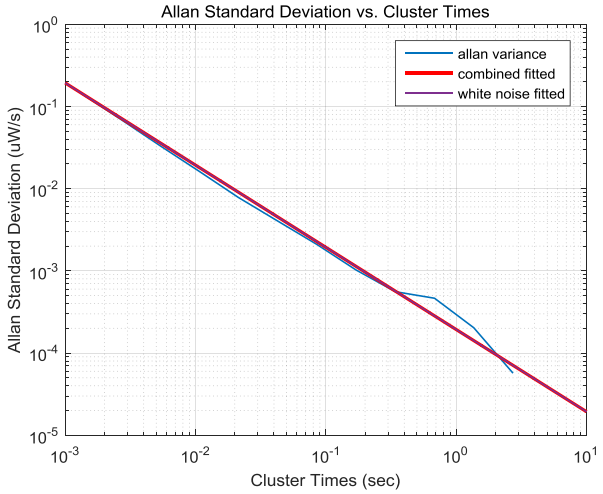

FIGURE 8. Allan variance of the RSS values received from one LED (5 kHz) on other frequencies (4.5 kHz) under the conditions of only one LED on and no ambient light interference.

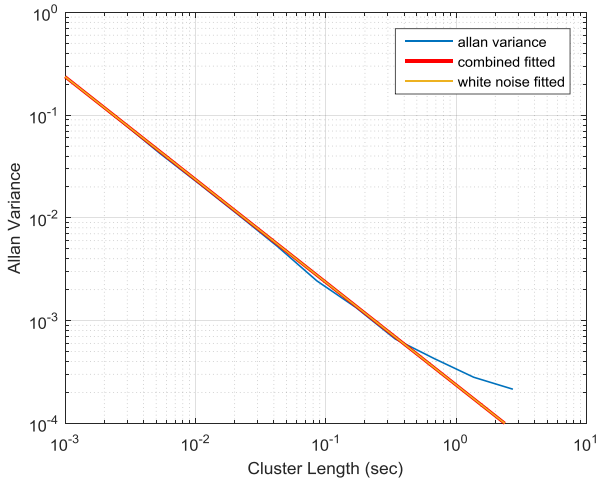

FIGURE 9. Allan variance of the RSS values received from one LED (5 kHz) on other frequencies (3.2 kHz) under the conditions of only one LED on and no ambient light interference.

TABLE 4. Noise vs. distance (2.84m).

LED	White Noise (N)	Random Walk (K)
5 kHz	0.02493	0.10276
3.2 kHz	0.02880	0.07571
1.8 kHz	0.04311	0.01207

Another test was conducted to further evaluate the performance of the Allan variance method. In this test, we moved the receiver 2 m away from its original location and maintained other parameters of the system. Three LEDs (1.8 kHz, 3.2 kHz, and 5 kHz) were tested again and the results are shown in TABLE 5. Both white noise and random walk decreased since both noises are positively related to the power of the received signals. However, the white noise component is still larger than the result of 'dark test'. It is because the dark current noise is unchanged while only the part of the LED's contribution became smaller.

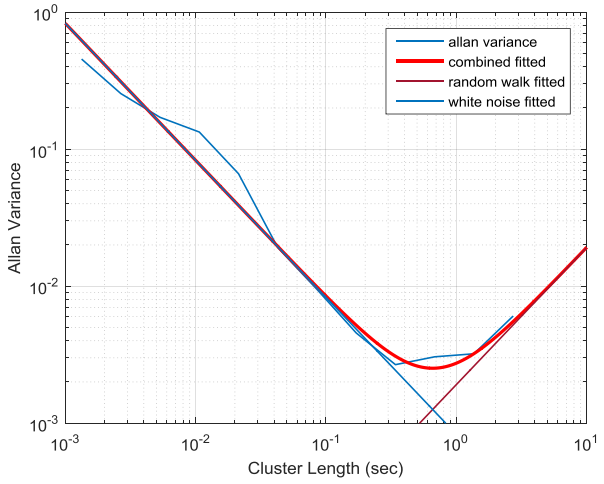

FIGURE 10. Allan variance of the RSS values received from one LED (3.2 kHz) under the conditions of only one LED on and no ambient light interference.

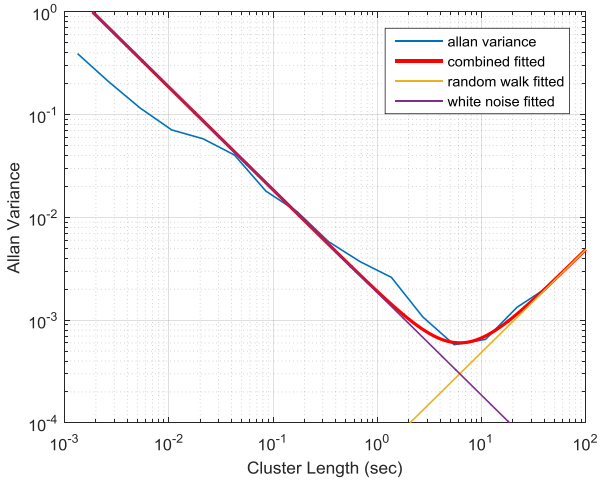

FIGURE 11. Allan variance of the RSS values received from one LED (1.8 kHz) under the conditions of only one LED on and no ambient light interference.

TABLE 5. Noise vs. distance (3.47m).

LED	White Noise (N)	Random Walk (K)
5 kHz	0.01409	0.01774
3.2 kHz	0.01439	0.01036
1.8 kHz	0.01711	0.00198

V. CONCLUSION

A novel scheme of noise measurement was proposed for the visible light system based on Allan variance. A practical visible light system was built and field tests were used to study VLC noise and evaluate the performance of the proposed scheme. From the results, two types of noise were observed. On short cluster time, white noise was the dominant noise component. On long cluster time, random walk was identified as the dominant noise, which has not yet been mentioned in former studies. From other results, the coefficient of white noise from 'dark test' was smaller than that when a LED light was on. And by increasing the distance between the receiver and LED light, both noise components were dropped.

REFERENCES

[1] H. Haas, L. Yin, Y. Wang, and C. Chen, "What is LiFi?" *J. Lightw. Technol.*, vol. 34, no. 6, pp. 1533–1544, Mar. 15, 2016.
[2] Y. Zhuang *et al.*, "A survey of positioning systems using visible LED lights," *IEEE Commun. Surveys Tuts.*, vol. 20, no. 3, pp. 1963–1988, 3rd Quart., 2018.
[3] D. Karunatilaka, F. Zafar, V. Kalavally, and R. Parthiban, "LED based indoor visible light communications: State of the art," *IEEE Commun. Surveys Tuts.*, vol. 17, no. 3, pp. 1649–1678, 3rd Quart., 2015.
[4] A. Sevincer, A. Bhattarai, M. Bilgi, M. Yuksel, and N. Pala, "LIGHTNETs: Smart lighting and mobile optical wireless networks—A survey," *IEEE Commun. Surveys Tuts.*, vol. 15, no. 4, pp. 1620–1641, 4th Quart., 2013.
[5] Y. Zhuang, Z. Syed, Y. Li, and N. El-Sheimy, "Evaluation of two WiFi positioning systems based on autonomous crowdsourcing of handheld devices for indoor navigation," *IEEE Trans. Mobile Comput.*, vol. 15, no. 8, pp. 1982–1995, Aug. 2016.
[6] Y. Zhuang, J. Yang, Y. Li, L. Qi, and N. El-Sheimy, "Smartphone-based indoor localization with Bluetooth low energy beacons," *Sensors*, vol. 16, no. 5, p. 596, Apr. 2016.
[7] J. Gancarz, H. Elgala, and T. D. C. Little, "Impact of lighting requirements on VLC systems," *IEEE Commun. Mag.*, vol. 51, no. 12, pp. 34–41, Dec. 2013.
[8] C.-H. Yeh, Y.-L. Liu, and C.-W. Chow, "Real-time white-light phosphor-LED visible light communication (VLC) with compact size," *Opt. Express*, vol. 21, no. 22, pp. 26192–26197, 2013.
[9] C. Luo, P. Casaseca-de-la-Higuera, S. McClean, G. Parr, and P. Ren, "Characterization of received signal strength perturbations using allan variance," *IEEE Trans. Aerosp. Electron. Syst.*, vol. 54, no. 2, pp. 873–889, Apr. 2017.
[10] A. J. C. Moreira, R. T. Valadas, and A. M. de Oliveira Duarte, "Optical interference produced by artificial light," *Wireless Netw.*, vol. 3, no. 2, pp. 131–140, 1997.
[11] T. Komine and M. Nakagawa, "Fundamental analysis for visible-light communication system using LED lights," *IEEE Trans. Consum. Electron.*, vol. 50, no. 1, pp. 100–107, Feb. 2004.
[12] B. Schneider and M. J. O. Strutt, "Theory and experiments on shot noise in silicon p-n junction diodes and transistors," *Proc. IRE*, vol. 47, no. 4, pp. 546–554, 1959.
[13] I. I. Taubkin, "Photoinduced and thermal noise in semiconductor p–n junctions," *Phys.-Uspekhi*, vol. 49, no. 12, p. 1289, 2006.
[14] F. Madani, G. Baghersalimi, and Z. Ghassemlooy, "Effect of transmitter and receiver parameters on the output signal to noise ratio in visible light communications," in *Proc. Iranian Conf. Electr. Eng. (ICEE)*, 2017, pp. 2111–2116.
[15] D. W. Allan, "Statistics of atomic frequency standards," *Proc. IEEE*, vol. 54, no. 2, pp. 221–230, Feb. 1966.
[16] N. El-Sheimy, H. Hou, and X. Niu, "Analysis and modeling of inertial sensors using Allan variance," *IEEE Trans. Instrum. Meas.*, vol. 57, no. 1, pp. 140–149, Jan. 2008.
[17] *IEEE Standard Specification Format Guide and Test Procedure for Linear, Single-Axis, Non-gyroscopic Accelerometers*, IEEE Standard 1293-1998, 1999.
[18] X. Niu *et al.*, "Using Allan variance to analyze the error characteristics of GNSS positioning," *GPS Solutions*, vol. 18, no. 2, pp. 231–242, Apr. 2014.
[19] *IEEE Standard Specification Format Guide and Test Procedure for Linear,Single-Axis, Nongyroscopic Accelerometers Corrigendum 1: Changes to Annex K and Annex L*, IEEE Standard 1293-1998/Cor 1-2008 (Corrigendum to IEEE Std 1293-1998), 2008, p. C1-3.
[20] E. Giard *et al.*, "Noise measurements for the performance analysis of infrared photodetectors," in *Proc. 22nd Int. Conf. Noise Fluctuations (ICNF)*, 2013, pp. 1–4.
[21] Y. Zhang, Y. Zhu, W. Xia, F. Yan, L. Shen, and Y. Wu, "Localization for visible light communication with practical non-Gaussian noise model," in *Proc. 9th Int. Conf. Wireless Commun. Signal Process. (WCSP)*, 2017, pp. 1–6.
[22] J. G. Proakis, *Digital Communications and Signal Processing*, 3rd ed. New York, NY, USA: McGraw-Hill, 1995.

[23] J. A. Barnes *et al.*, "Characterization of frequency stability," *IEEE Trans. Instrum. Meas.*, vol. IM-20, no. 2, pp. 105–120, May 1971.

[24] P. Lou, H. Zhang, X. Zhang, M. Yao, and Z. Xu, "Fundamental analysis for indoor visible light positioning system," in *Proc. 1st IEEE Int. Conf. Commun. China Workshops (ICCC)*, Aug. 2012, pp. 59–63.

LUCHI HUA received the B.S. degree from the Harbin Institute of Technology, Harbin, China, in 2014, and the M.S. degree from Southeast University, Nanjing, China, in 2018, where he is currently pursuing the Ph.D. degree in microelectronics and solid state electronics. His current research interests include wireless communication and its applications to the field of indoor positioning.

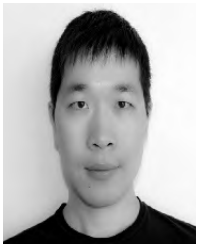

YUAN ZHUANG (M'16) received the bachelor's degree in information engineering and the master's degree in microelectronics and solid-state electronics from Southeast University, Nanjing, China, in 2008 and 2011, respectively, and the Ph.D. degree in geomatics engineering from the University of Calgary, Canada, in 2015. Since 2015, he has been a Lead Scientist at Bluvision Inc., Fort Lauderdale, FL, USA. He was a Baseband Engineer with CSR Technology, Shanghai Co., Ltd., Shanghai, China, and an Algorithm Designer with Trusted Positioning Inc., Calgary, Canada. Until now, he has co-authored over 35 academic papers and 11 patents. His current research interests include real-time location system, personal navigation system, wireless positioning, multi-sensors integration, Internet of Things (IoT), and machine learning for navigation applications. He has received over 10 academic awards. He is a reviewer of several IEEE journals and the Guest Editor of the IEEE Internet of Things Journal and IEEE Access.

LONGNING QI was born in Zhejiang, China, in 1979. He received the B.S. degree in communication engineering, and the M.S. and Ph.D. degrees in microelectronics and solid-state electronics from Southeast University, Jiangsu, China, in 2001, 2003, and 2008, respectively. He has been with the National ASIC System Engineering Research Center, Southeast University, China, since 2008. His current research interests include low power design, GNSS tracking, sensor fusion, and indoor location.

JUN YANG (M'15) received the bachelor's, master's, and Ph.D. degrees from Southeast University in 1999, 2001, and 2004, respectively. He is currently a Professor with the National ASIC Center, Southeast University, Nanjing, China. His research interests include near threshold circuit design and ultra-low power indoor/outdoor position algorithm and chips. He owned three US patents, 1 EU patent, over 40 Chinese patents, and co-authored over 50 academic papers. He has supervised and graduated over 30 master's and Ph.D. students. He is a recipient of several national awards, including the State Science and Technology Awards.

LONGXING SHI (SM'06) received the Ph.D. degree in microelectronics from Southeast University in 1988. He is currently a Professor and the Dean of the Electrical Science and Technology School, Southeast University. He has published over 120 technical papers in conferences and journals, and received over 200 Chinese invention patents and 11 USA patents. His research interests include system-on-chip design, RF and mixed-signal integrated circuit design.